Supporting Information

PCDTBT: From polymer photovoltaics to light-emitting diodes by side chain-controlled luminescence

Florian Lombeck[1,2‡], Dawei Di[1‡], Le Yang[1], Lorenzo Meraldi[1], Stavros Athanasopoulos,[1] Dan Credgington[1], Michael Sommer[2,3,4], Richard H. Friend[1*]*

Materials

P0 and **P100** as well as the monomers were synthesized according to the literature.[S1-S3] Solvents were purchased from Sigma Aldrich and used as received.

*Syntheses of **P30-P90***

The monomers (ratios and weights are given in Table S1) were placed in a 10 ml microwave vial. Toluene was added to yield a $Cbz(Bpin)_2$ concentration of 0.05 M. 2 ml K_2CO_3 (2M) and 2 drops Aliquat 336 were added. The solution was purged with nitrogen for 20 min. Pd_2dba_3 (0.5 mol%) and SPhos (2mol%) were added. The reaction mixture was heated under vigorous stirring in a microwave reactor at 80°C for 3h. After the reaction was completed, the mixture was

allowed to cool to room temperature. The aqueous phase was removed and THF was added to dissolve solid components. The resulting polymer was precipitated in methanol, filtered and washed by successive Soxhlet extraction with methanol, acetone, hexanes, and chloroform. The chloroform fraction was collected, filtered through a pad of silica, dried under vacuum and used for this study.

Table S1. Monomer feed ratios for the individual terpolymers **P0 - P100**.

Polymer	**Br_2TBT [mg / µmol]**	**Br_2hex-TBT [mg / µmol]**	**Cbz(Bpin)$_2$ [mg / µmol]**	**Yield (CF-fraction) [mg / %]**
P0	49.9 / 109.0	---	71.7 / 109.0	32.1 / 42
P30	28.3 / 61.7	16.5 / 26.4	57.9 / 88.1	31.8 / 48
P40	31.9 / 69.6	29.1 / 46.4	76.3 / 116	41.1 / 46
P50	30.6 / 66.8	41.8 / 66.8	87.8 / 133.6	55.7 / 53
P60	18.8 / 41.1	38.9 / 62.1	68.1 / 103.5	49.0 / 59
P70	18.2 / 39.8	58.1 / 92.8	87.2 / 132.6	76.1 / 70
P80	12.1 / 26.4	66.0 / 105.4	86.6 / 131.8	75.0 / 68
P90	6.5 / 14.2	80.1 / 127.8	93.4 / 142	89.7 / 74
P100	---	61.5 / 98.2	64.6 / 98.2	73.5 / 86

Experimental Details

GPC measurements. GPC measurements were carried out on an Agilent PL-GPC220 instrument equipped with a RI detector at 150 °C in 1,2,4-tricholorobenzene (TCB) and calibrated relative to polystyrene at a flow rate of 1.0 ml/min.

NMR Spectroscopy. ^{1}H NMR spectra were recorded at 500.13 MHz on a Bruker Avance III 500 spectrometer using a 5 mm $^{1}H/^{13}C/^{19}F/^{31}P$ gradient probe at 120°C. $C_2D_2Cl_4$ was used as solvent and the spectra were referenced on the residual solvent peak ($\delta(^{1}H)$ = 5.98 ppm).

UV-vis spectroscopy. UV-vis spectra were recorded on a Lambda 650 S spectrometer from Perkin Elmer in film or in chlorobenzene solutions (c = 0.02 mg/ml).

Differential Scanning Calorimetry. DSC measurements were carried out on a DSC 204 F1

(Netzsch) under a nitrogen atmosphere. Heating and cooling rates were 10 K/min. The mass of the sample for each measurement was approximately 3-5 mg.

Ultraviolet photoelectron spectroscopy. For UPS measurements 7 nm of chromium and 70 nm of gold were evaporated on top of a clean silicon substrate. The ~10 nm - 15 nm thin polymer film was deposited via spin coating. After thermal annealing at 160°C for 10min. in a nitrogen-filled glovebox, the films were transferred into an ultrahigh vacuum chamber (ESCALAB 250Xi). UPS measurements were carried out using a pumped He gas discharge lamp emitting He I radiation ($h\nu$ = 21.2 eV).

Photoluminescence quantum efficiency. The measurement is carried out on films deposited on quartz glass (Spectrosil 2000) or chlorobenzene solutions (0.02 mg/ml) in a Hellma quartz cuvette (1 mm beam path) via excitation of the sample with a 523 nm laser. The sample is placed inside an integrating sphere. The integrating sphere´s inside is reflective and purged with nitrogen. The light collected from the integrating sphere is coupled through a fiber into a spectrometer (Shamrock SR303i, Andor Technologies). Three individual measurements were

performed to calculate the quantum yield ϕ according to DE MELLO *et al.*[S4] In the ON measurement the laser is focused on the film directly, whereas in the OFF measurement the laser does not hit the sample but the reflective wall of the integrating sphere. The background is subtracted by measuring the integrating sphere without sample to account for impurities inside the sphere. The PLQE is calculated by the difference in the area of the laser peak of all three measurements, which gives the amount of photons absorbed by the film, and the difference in the signal area of the emission peak, giving the number of photons emitted.

OPV Device fabrication. Photovoltaic devices were fabricated in the standard ITO | PEDOT:PSS | polymer:PCBM | Ca/Al layer sequence. ITO on glass anodes were first cleaned with acetone and isopropanol, followed by oxygen plasma treatment. A ~40 nm thick PEDOT:PSS was spin-coated onto the plasma-treated substrates, annealed at 230 °C for 10 min and transferred into a nitrogen-filled glovebox for the subsequent fabrication steps.

$PC_{71}BM$ blend OPV devices. Photoactive layers were spin-cast from 1,2.dichlorobenzene (o-DCB)-solution ($PC_{71}BM$, 48 mg/ml in o-DCB and polymer, 12 mg/ml, were mixed in a 1:1 ratio to give the active blend mixture) in air to give ~90 nm thick films. Finally, after keeping the films at 10^{-7} mbar for at least 12h, an Aluminum electrode (100 nm) was evaporated at ~10^{-7} mbar and the devices were encapsulated using an epoxy resin.

P3HT blend OPV devices. The polymer and P3HT were mixed in a 1:1 ratio in chlorobenzene and additional 10% 4-bromoanisole was added.[S5] The final blend mixture was 15 mg/ml and spun to give an active layer of ~65-70 nm. After thermal treatment (10 min at 240°C), an Aluminum electrode (100 nm) was evaporated at 10^{-7} mbar, the devices were additionally annealed at 140°C for 3min prior to encapsulation with an epoxy resin.

OPV device testing. Device EQE was measured using a tungsten lamp with a monochromator at intensities of ~1 mWcm^{-2}. Short circuit currents were recorded using a Keithley 237 source meter. The current–voltage characteristics of the device were measured under simulated 100 mW cm^{-2} AM 1.5 illumination using an Abet Technology solar simulator. The spectral mismatch of the simulator was calibrated to a silicon reference cell.

Atomic Force Microscopy. AFM capturing was carried out on a Veeco Dimension 3100 AFM, operated in tapping mode.

OLED fabrication. ITO-patterned substrates were cleaned by ultrasonication in acetone and IPA for 10 min respectively, before being oxygen plasma-etched for 10 min. PEDOT:PSS (30 nm) was filtered and spincoated onto the substrates in air, and annealed under nitrogen flow at 200^{o}C for 20 min. Poly(9,9-dioctylfluorene-co-N-(4-butylphenyl)diphenylamine) (TFB) was spincoated from anhydrous toluene solution on top of the PEDOT:PSS in a nitrogen-filled glovebox, followed by annealing of the films at 200^{o}C for 20 min. P0-P100 polymers were each dissolved in anhydrous chlorobenzene, and spincoated onto the TFB through a PTFE filter, followed by annealing of the films at 150^{0}C for 10 min. Resulting TFB films were ~30 nm thick while the emissive layer is ~70-100 nm thick. ~40 nm of 2,2′,2"-(1,3,5-Benzinetriyl)-tris(1-phenyl-1-H-benzimidazole) (TPBi) was spincoated from an anhydrous solution in methanol onto the emissive layer, followed by annealing at 60^{0}C for 10 min. Finally lithium fluoride (0.6 nm) and aluminium (100 nm) were subsequently evaporated under vacuum (3×10^{-6} mbar) through a shadow mask, with typical pixel area of 5.25 mm^2. Electrical contacts were attached

thereforeafter, and the devices were encapsulated with clear glass slides. Devices were stored in a glovebox for 12 h before characterization.

OLED characterization. Electroluminescence (EL) spectra were collected using an optical fibre attached to the Ocean Optics USB 2000 spectrometer. A silicon photodiode with an active area of 100 mm^2 collects electroluminescence signal (photons) from a LED device, and the distance between the photodiode and the LED is controlled and recorded. A Keithley 2400 source meter supplied the voltage input, and a Keithley 2000 source meter measures the output of the photodiode.

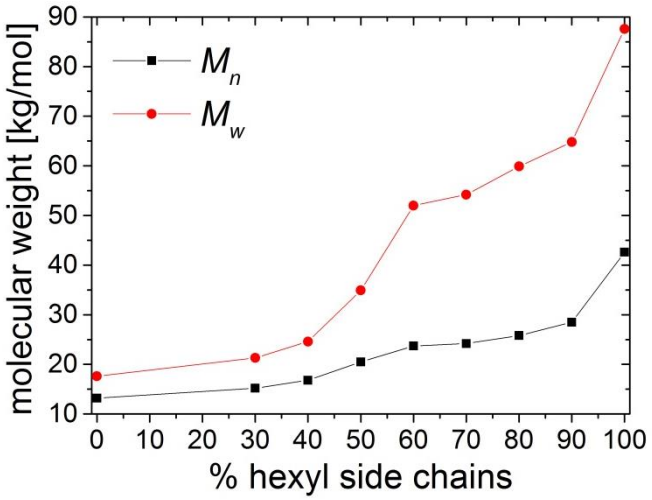

Figure S1. Correlation of molar mass of the chloroform fraction and hexyl side chain density.

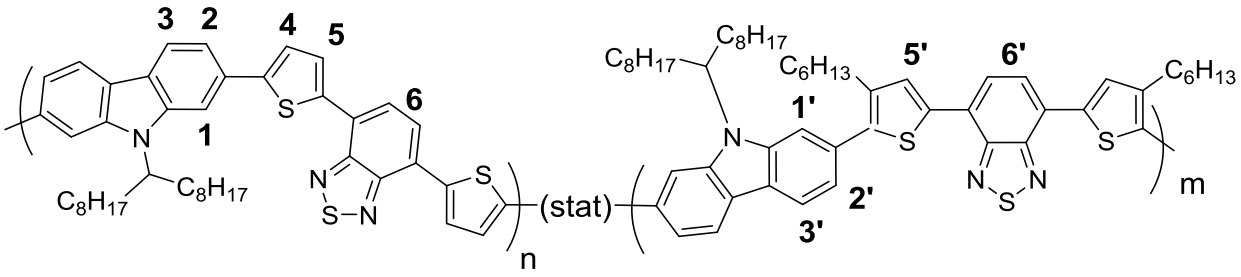
3
2
4
5
6
1
N
S
N
S
N
S
n
C8H17
C8H17
(stat)
C8H17
C8H17
C6H13
5'
6'
1'
2'
3'
C6H13
m

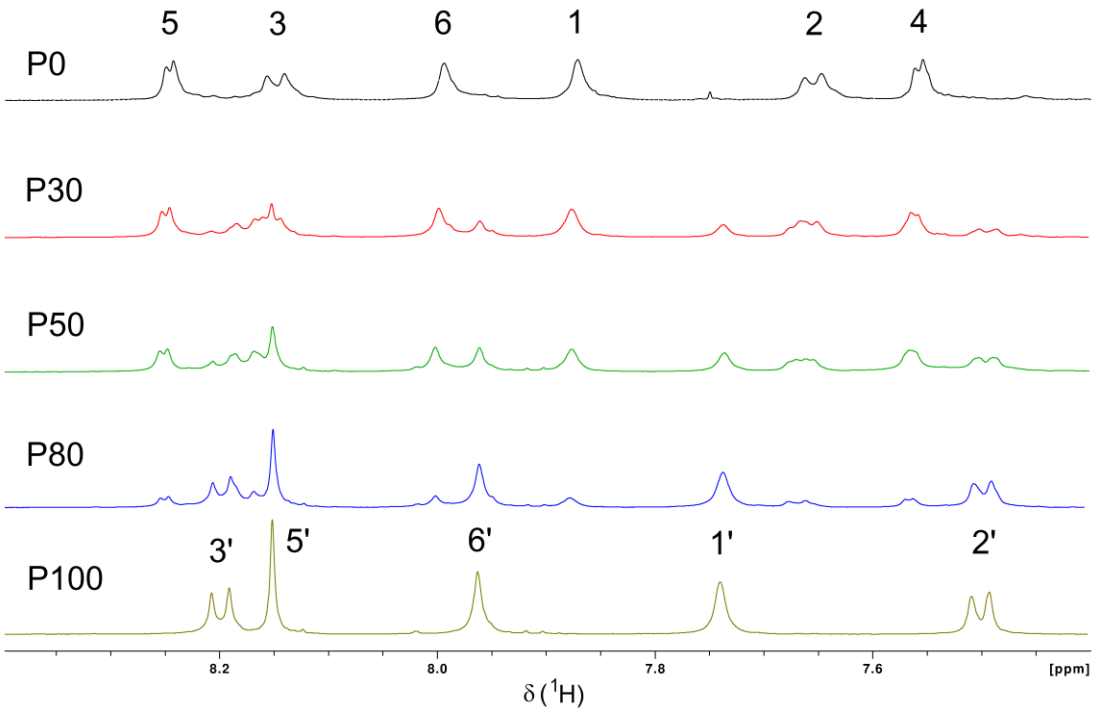
5
3
6
1
2
4
P0
P30
P50
P80
P100
3'
5'
6'
1'
2'
8.2
8.0
7.8
7.6
[ppm]
δ (1H)

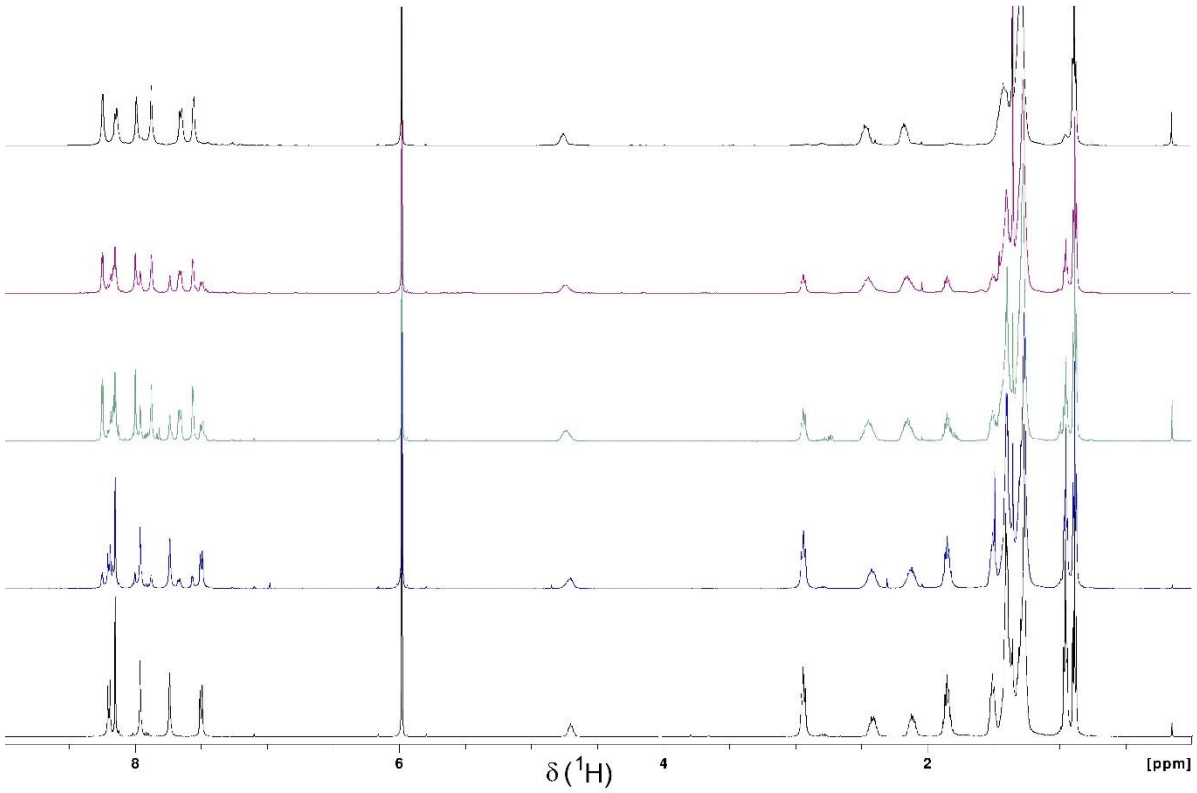

Figure S2. ^{1}H NMR spectra of **P0, P30, P50, P80** and **P100.** Top: aromatic region with signal assignments, bottom: full ppm range. Spectra were taken in $C_2D_2Cl_4$ at 120°C.

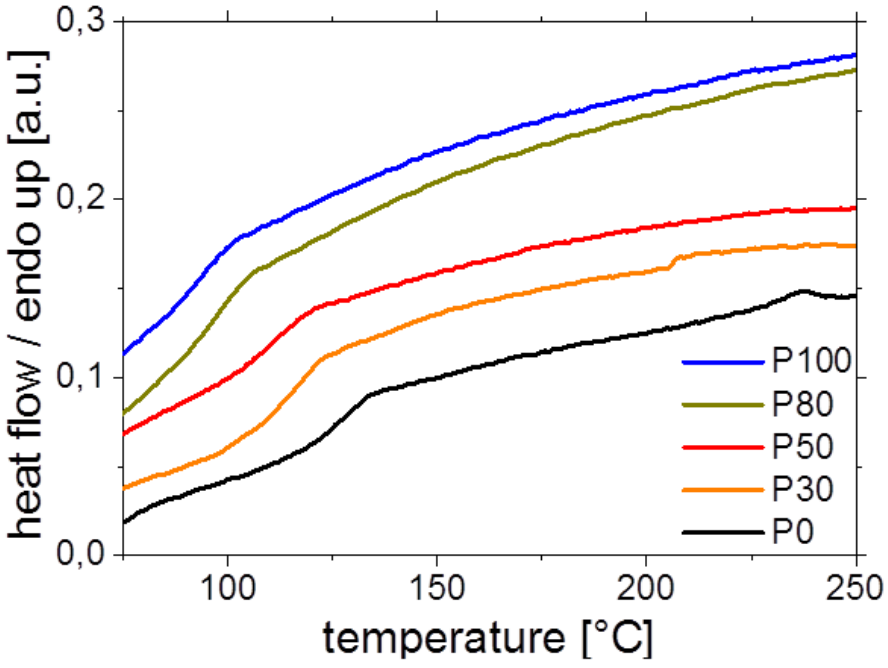

Figure S3. DSC curves of **P0** (black), **P30** (orange), **P50** (red), **P80** (green) and **P100** (blue).

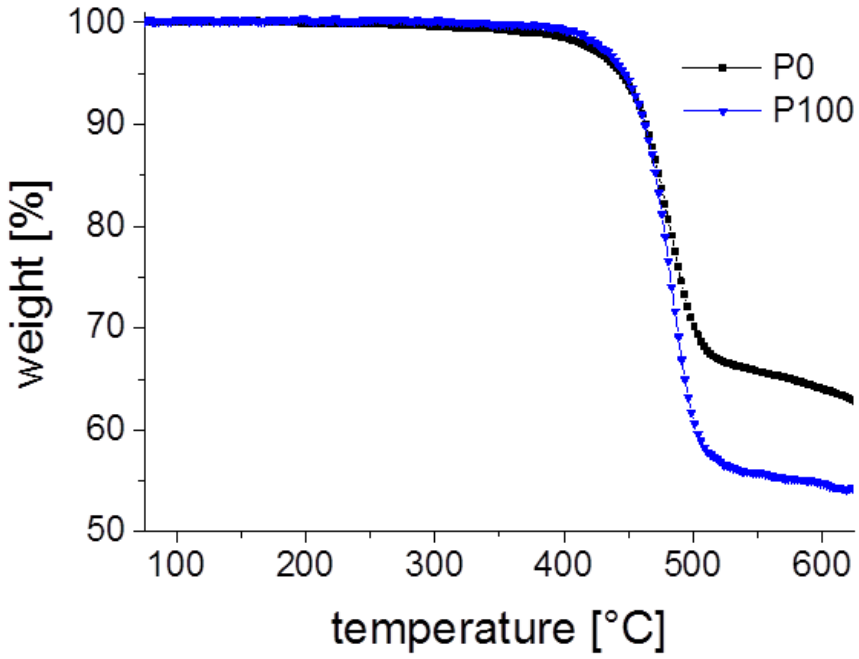

Figure S4. Thermogravimetric curve of **P0** (black) and **P100** (blue). Heating rate was 10K/min under a nitrogen atmosphere. No significant degradation takes place below 400°C.

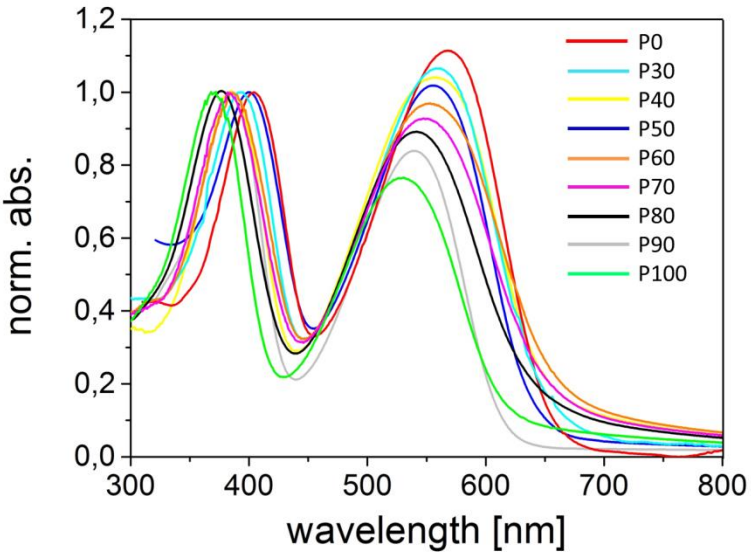

Figure S5. UV-vis spectra of all terpolymers **P0 - P100** in chlorobenzene (c= 0.02 mg/ml).

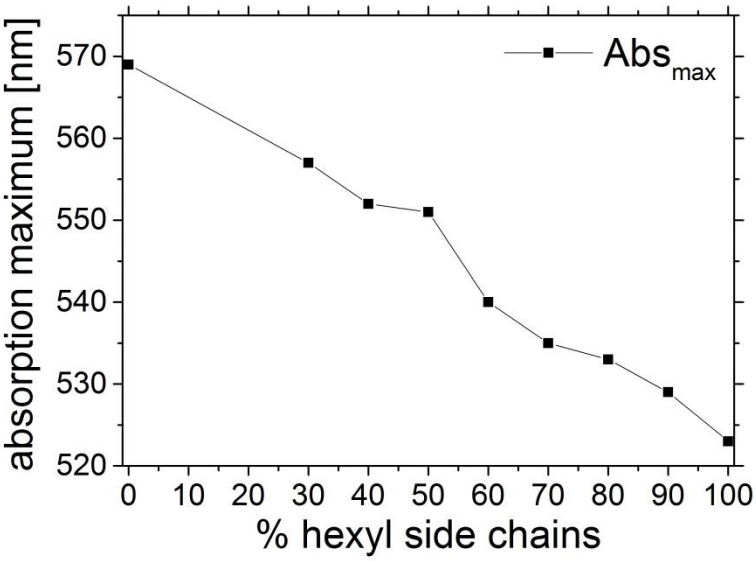

Figure S6. Correlation of charge-transfer band absorption maximum in solution and hexyl side chain density.

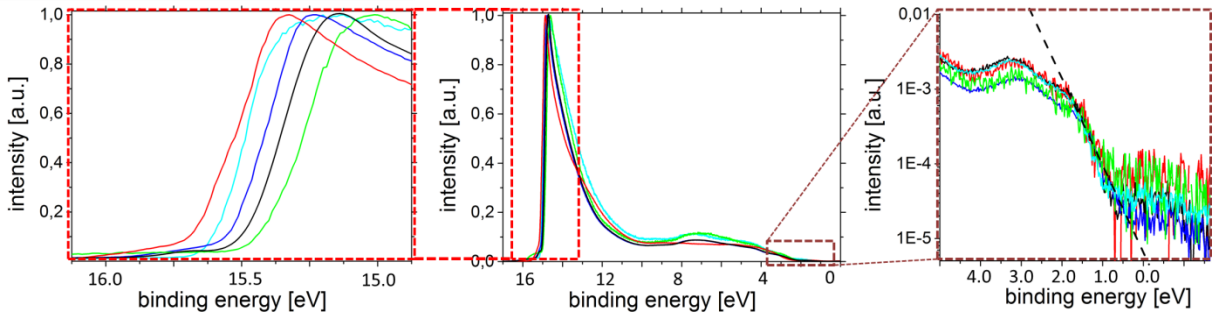

Figure S7. UPS-spectra of **P0** (green), **P30** (black), **P50** (blue), **P80** (cyan) and **P100** (red).

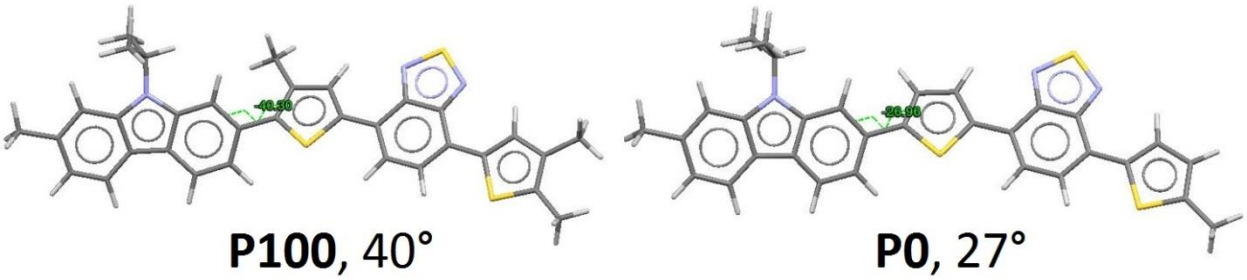

Figure S8. Calculated dihedral angles between the TBT and the CBZ unit of the repeating unit of P100 (left) and P0 (right). The hexyl side chain is substituted by a methyl group for simplification of DFT calculations.

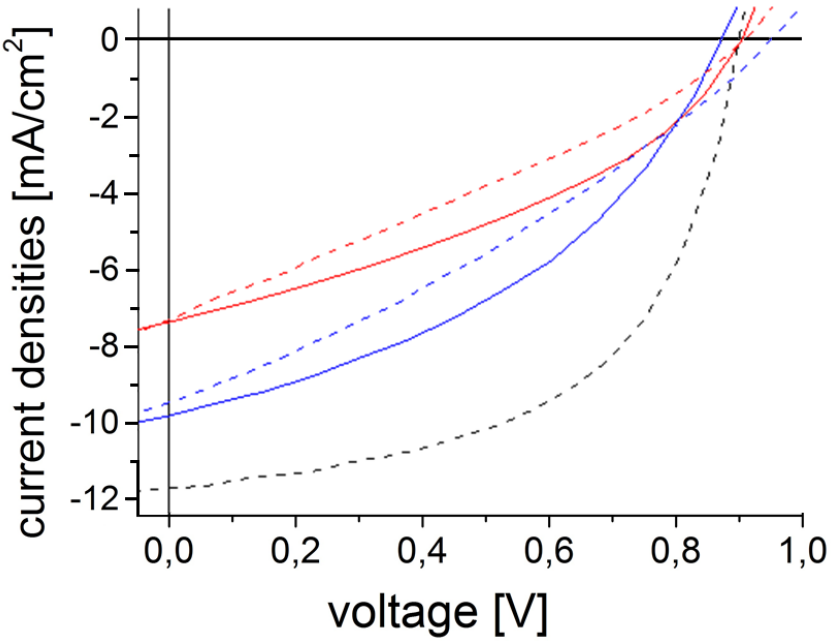

Figure S9. Molecular weight dependence of OPV characteristics of **P100** (red), **P50** (blue) and **P0** (black). Dashed lines represent OPV devices made from comparable molecular weights (M_n 22-24 kg/mol), while solid lines represent OPV devices fabricated from the highest obtained molecular weight polymers (**P100** 46 kg/mol, **P50** 36 kg/mol, both obtained from the chloroform fraction). As can be seen, mostly the fill factor is influenced by variation of the molar mass with increased *FF* upon increased MW while V_{oc} and J_{sc} are basically unaffected.

The series of PCDTBT in blends with P3HT was tested in regard to controlling miscibility and therefore morphology. In such a combination PCDTBT acts in OPV devices as an electron acceptor with a P3HT donor counterpart. Previously, we observed that usage of a hexylated TBT monomer in both F8TBT[S6] as well as PCDTBT[S7] prevents microphase separation in their corresponding block copolymers with P3HT. As the classical PCDTBT without side chains at the TBT unit is poorly soluble which complicates processibility especially for larger molecular weights[S8], we envisioned that balancing the amount of hexyl side chains could lead to controllable phase separation and hence domain size and sufficient solubility. This is indeed

indicated by AFM analysis (Figure S7). After annealing above the melting transition of P3HT ($T_{m(P3HT)}$ = 225°C), domain size clearly decreases with increasing hexyl-TBT incorporation, suggesting better miscibility with P3HT due to increasingly similar backbones.

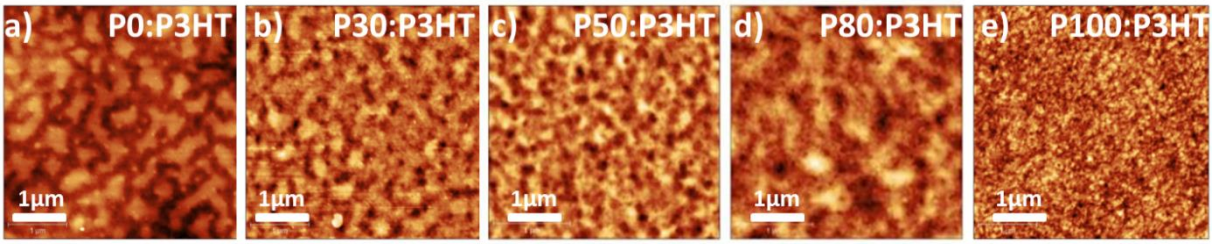

Figure S10. AFM (height) images of polymer blends: a) **P0**:P3HT (1:1); b) **P30**:P3HT (1:1); c) **P50**:P3HT (1:1); d) **P80**:P3HT (1:1) and e) **P100**:P3HT (1:1).

OPV devices were fabricated using a 1:1 PCDTBT:P3HT ratio (by weight). Active layers were spun from chlorobenzene with 10% 4-bromoanisol added.[S5] After deposition, the devices were thermally annealed prior to electrode evaporation. A decreasing OPV device performance upon increasing side chain density was found (Figure S8 and Table S2) with **P0** in combination with P3HT giving a PCE of 0.84% and a remarkable high open-circuit voltage of up to 1.26 V, while the combination of **P100** and P3HT results in a PCE of 0.54 %. **P30**, **P50** and **P80** give, combined with P3HT, intermediate PCEs of 0.68%, 0.56% and 0.57%, respectively. Due to pronounced shoulders at lower energies, the shape of the EQE curves indicates an increased P3HT crystallinity upon a lower hexyl chain density on the PCDTBT. However, an increased melting enthalpy for **P0**:P3HT compared to **P100**:P3HT could not be found.[S7]

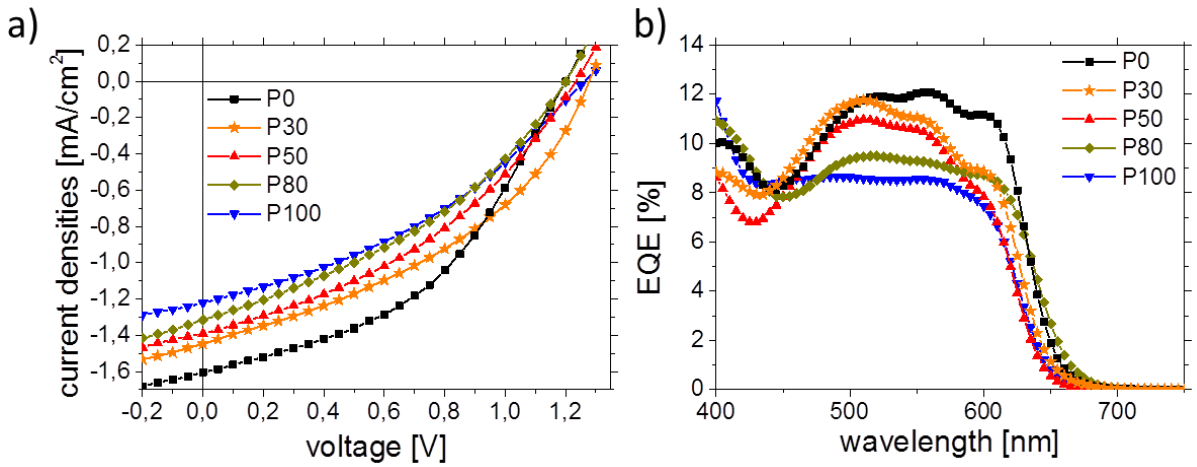

Figure S11. a) *J-V*- and b) EQE-curves of OPV devices made from polymer blends **P0-P100**:P3HT in standard device architecture (glass | ITO | PEDOT:PSS | polymer:P3HT | Al).

Table S2. OPV device characteristics of polymer:P3HT devices.

Polymer	V_{oc} **[V]**	J_{sc} **[mA/cm²]**	***FF*** **[%]**	**PCE [%]**
P0	1.13 ± 0.13 (1.26)	1.61 ± 0.21	46 ± 2	0.84
P30	1.21 ± 0.07 (1.28)	1.45 ± 0.14	39 ± 2	0.68
P50	1.10 ± 0.13 (1.25)	1.38 ± 0.31	37 ± 1	0.56
P80	1.14 ± 0.13 (1.27)	1.31 ± 0.18	38 ± 3	0.57
P100	1.20 ± 0.05 (1.23)	1.23 ± 0.38	36 ± 1	0.53

Quenching experiments with $PC_{71}BM$ show an efficient PL quenching >99% by the addition of 10 wt.-% $PC_{71}BM$ only. Interestingly, the relatively high PL of **P100** (PLQE= 19%) is quenched completely upon addition of 2 wt.-% $PC_{71}BM$ only, while the PL of **P0** is thoroughly quenched upon addition of 10 wt.-% $PC_{71}BM$ (Table S2 and Figure S9). These results indicate some extend of well intermixed phases and a high interfacial area of **P100** and $PC_{71}BM$, whereas **P0**

might form larger domains as a consequence of increased ability to interact *via* π-π stacking, hence due to lower solubility and pre-aggregation.

Table S3. Values for PLQE quenching experiment.

wt.-% $PC_{71}BM$	**PLQE (P100) [%]**	**PLQE (P0) [%]**
0	18,3	4,3
0,1	4,2	2,6
0,5	2	2
1	1,3	1,39
2	0,19	0,82
5	0,1	0,42
10	0	0,0289

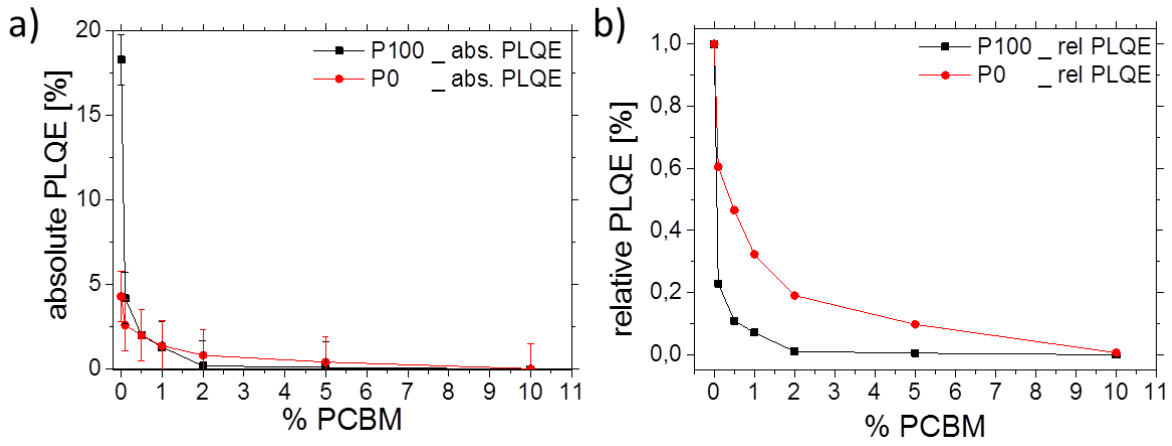

Figure S12. Quenching experiments with $PC_{71}BM$. a) absolute and b) relative PLQE.

SI References

(S1) Lévesque, I.; Bertrand, P.; Blouin, N.; Leclerc, M.; Zecchin, S.; Zotti, G.; Ratcliffe, C. I.; Klug, D. D.; Gao, X.; Gao, F. *Chem. Mater.* **2007**, 17, 2128–2138.

(S2) Lombeck, F.; Komber, H.; Gorelsky, S. I.; Sommer, M. Identifying Homocouplings as Critical Side Reactions in Direct Arylation Polycondensation. *ACS Macro Lett.* **2014**, *3*, 819–823.

(S3) Kim, J.; Kwon, Y. S.; Shin, W. S.; Moon, S.-J.; Park, T. Carbazole-Based Copolymers: Effects of Conjugation Breaks and Steric Hindrance. *Macromolecules* **2011**, *44*, 1909–1919.

(S4) DeMello, J. C. ; Wittmann, H. F.; Friend, R. H. An improved experimental determination of external photoluminescence quantum efficiency. *Adv. Mater.* **1997**, *9*, 230–232.

(S5) Liu, X.; Huettner, S.; Rong, Z.; Sommer, M.; Friend, R.H. Solvent additive control of morphology and crystallization in semiconducting polymer blends. *Adv. Mater.* **2012**, *24*, 669-674.

(S6) Sommer, M.; Komber, H.; Huettner, S.; Mulherin, R.; Kohn, P.; Greenham, N.; Huck, W. Synthesis, purification and characterization of well-defined all-conjugated diblock copolymers PF8TBT-b-P3HT. *Macromolecules* **2012**, *45*, 4142-4151.

(S7) Lombeck, F.; Komber, H.; Sepe, A.; Friend, R. H.; Sommer, M. Enhancing phase separation and photovoltaic performance of all-conjugated donor acceptor block copolymers with semifluorinated side chains. *Macromolecules* **2015**, *48*, 7851-7860.

(S8) Kingsley, J. W.; Marchisio, P. P.; Yi, H.; Iraqi, A.; Kinane, C. J.; Langridge, S.; Thompson, R. L.; Cadby, A. J.; Pearson, A. J.; Lidzey, D. G.; Jones, R. A. L.; Parnell, A. J. Molecular weight dependent vertical composition profiles of PCDTBT:$PC_{71}BM$ blends for organic photovoltaics. *Sci. Rep.* **2014**, *4*, 1–7.